Experimental determination of section sensitivity profiles and image noise in electron beam computed tomography[a)]

Cynthia H. McCollough,[b)] Kalpana M. Kanal, Nicholas Lannutti, and Kelly J. Ryan
Department of Diagnostic Radiology, Mayo Clinic and Mayo Foundation, Rochester, Minnesota 55905

(Received 9 September 1998; accepted for publication 3 December 1998)

To determine the effect of continuous-volume scanning (CVS) on *z*-axis resolution, section sensitivity profiles were measured on an electron beam computed tomography (CT) scanner and compared with those obtained using the step-volume scanning (SVS) mode. A steel bead was imaged using different scan parameters, and the mean CT number over the bead was plotted against the *z*-axis position to determine section sensitivity profiles. From these profiles, full width at half maximum (FWHM), full width at tenth maximum (FWTM), and full width at tenth area (FWTA) were calculated. A uniform water phantom was imaged to measure noise. To determine the visual significance of changes in the section sensitivity profile, a section thickness and contiguity phantom was imaged. All section sensitivity profiles measured had an FWHM value within 0.5 mm of the nominal scan width. The FWTM and FWTA values increased with the CVS mode compared with the SVS mode. This broadening of the section sensitivity profiles was most significant with larger collimator widths. However, use of smaller collimator widths increased image noise. When all other parameters remained constant, increasing the exposure time to reduce image noise did not affect the section sensitivity profile. The CVS mode produced wider section sensitivity profiles than the SVS mode. This effect was minimized when the smallest collimator width was used, but at the expense of increased image noise.
[S0094-2405(99)02202-6]

Key words: CT image quality, CT physics, spiral CT technology, electron beam CT

I. INTRODUCTION

Electron beam computed tomography (CT) equipment differs significantly from that of conventional CT scanning. X-rays are produced by scanning a focused electron beam about a tungsten target positioned in a semicircle below the patient. In this manner, mechanical motion within the gantry is eliminated and exposure times as low as 50 and 100 ms are made possible.[1–5]

The two modes of operation for an electron beam CT scanner are the single-slice and multislice modes. The single-slice mode of operation utilizes one of four tungsten targets and the high-resolution detector ring in conjunction with additional collimation to acquire images having scan widths between 1.5 and 10 mm. In the multislice mode of operation, the four tungsten target rings and two detector rings can be utilized to acquire 2, 4, 6, or 8 scans without movement of the patient table. In both the single-slice and multislice acquisition modes, the rapid scan acquisition times (0.1 and 0.05 s, respectively) can be used in various ways, depending on the clinical application. To reduce image noise, multiple 0.1 or 0.05-s scans can be averaged before image reconstruction. Four different data acquisition protocols can be used and are referred to as the movie, flow, step-volume, and continuous-volume scanning modes. The discussion in this article is restricted to the single-slice step-volume and continuous-volume scanning modes.

In the step-volume scanning (SVS) mode, the scanner acquires cross-sectional images at various levels throughout a volume of anatomy in a manner analogous to the operation of a conventional CT scanner. The patient table moves a specified distance (table increment) after each level is acquired, with an interscan delay on the order of 1 s. The table increment is typically equal to or larger than the scan width (nominal width of the reconstructed image, typically the full width at half maximum of the section sensitivity profile).

The collimator width (1.5, 3, or 6 mm) represents the nominal width of the detected x-ray beam at isocenter. For the 1.5- and 6-mm widths, the prepatient collimator openings are wider than the postpatient collimator openings in order to accommodate the cone-beam geometry of the scanner.

The exposure time represents the cumulative x-ray exposure time and is some integral multiple of 0.1-s exposures. For example, a 0.4-s exposure is actually four individual 0.1-s x-ray exposures. A 0.116-s intersweep delay occurs between repeat exposures and must be accounted for when calculating table speed.

In the continuous-volume scanning (CVS) mode, the table is moved continuously during data acquisition, similar to spiral CT. However, unlike spiral CT, during each extremely short scan time (0.1 s), the table moves a distance that is typically much shorter than the scan width; thus, each individual 0.1-s scan is essentially free of table motion artifact. Longer exposure times, which represent the sum of discrete 0.1-s scans, are the linear superposition of multiple scans acquired at small *z*-axis intervals. This may blur structures that change along the *z* axis within the cumulative exposure time, but it does not produce notable image artifacts. Thus, the interpolation algorithms used to reduce table motion ar-

tifact in spiral CT, which modify the projection data before image reconstruction so that they correspond to a single *z*-axis position, are not used in the normal CVS reconstruction. When the distance traveled during one scan time (0.1 s) approaches the scan width (i.e., pitch approaches 1), interpolation algorithms similar to those used in spiral CT must also be used in electron beam CT to reduce table motion artifacts. The overlapped and cone-beam reconstruction algorithms include such table motion corrections but were not studied in this article, as they are not routinely used in clinical practice. This is due to their longer reconstruction times and the less frequent use of 0.1- and 0.2-s exposure times, which produce higher noise images.

In the CVS mode, the table speed is not directly user selectable, but is rather determined by the user's choice of table increment and exposure time; table speed (mm/s) $=$table increment (mm) / (0.116 s $\times$ number of 0.1-s exposures). For example, a 6-mm table increment and 0.4-s exposure (four 0.1-s exposures) result in a table velocity of 12.9 mm/s. Terms such as table speed and pitch are not used by the electron beam scanner software. Instead, the user specifies the examination parameters in terms of desired (nominal) scan width, table increment, collimation width, and exposure time.

Unlike spiral CT systems, the current electron beam scanner software does not support rebinning the projection data to reconstruct nominal-scan-width images at any *z*-axis position. Instead, images are reconstructed only at an interval equal to the table increment or, in the overlapped or cone-beam CVS modes, at an interval equal to half of the table increment.

The purpose of this study was to determine the effect of the CVS mode of operation on *z*-axis resolution and image noise and to compare these measures to the standard SVS mode of operation. Specifically, we sought to determine the effect of parameter selection on section sensitivity profile width and image noise.

II. METHODS

A 0.25-mm steel bead embedded in foam and stabilized within an acrylic housing (model 76-412, Nuclear Associates, Carle Place, NY) was used to measure the section sensitivity profiles of an electron beam CT scanner (Evolution XP, Imatron, Inc., S. San Francisco, CA, marketed by Siemens Medical Systems). The bead phantom was placed on the patient table, and its center (the position of the bead) was aligned with the scanner's external axial, coronal, and sagittal lasers. Scans were acquired at 130 kVp and 640 mA (both parameters are fixed for electron beam CT scanners) with the SVS and CVS modes of operation, as detailed below.

In the SVS mode, scans were acquired with use of different collimator widths (1.5, 3, and 6 mm) and exposure times (0.4 and 1.4 s). A volume with length equal to three times the scan width was centered on the bead and imaged at 0.5-mm intervals to provide bead attenuation data along the *z* axis (that is, the section sensitivity profile). In the SVS mode of operation, these images were obtained sequentially within a single acquisition (scan run).

In the CVS mode, scans were acquired with different scan widths (1.5, 3, 6, 8, and 10 mm), table increments (1.5, 3, 6, 8, and 10 mm; matched respectively to scan width, as is done clinically for contiguous volume imaging), collimator widths (1.5, 3, and 6 mm), and exposure times (0.4, 0.6, and 1.4 s). Scans of a water phantom 25.4 cm in diameter were acquired for all of the SVS and CVS parameters to determine image noise.

To determine the section sensitivity profile, image data must be acquired with a sufficient sampling frequency along the *z* axis. An interval of 0.5 mm was used for this study. In the CVS mode, the table increment and exposure time determine the velocity of the patient table. Thus, a 0.5-mm increment would significantly decrease the table velocity and result in a section sensitivity profile similar to that produced with no table motion. Such data would not adequately describe the section sensitivity profile for images in which the table increment equals the scan width (1.5–10 mm), which is typical of clinical examinations. Thus, it is not possible to obtain image data for CVS section sensitivity profiles by using a single acquisition and reconstructing images at a 0.5-mm increment. Instead, a more cumbersome acquisition sequence was devised to obtain adequate spacing (0.5 mm) along the *z* axis while maintaining clinically relevant scan parameters. In this scheme, two images were obtained in a single acquisition with the table increment set equal to the scan width. After each acquisition, the starting table position was changed 0.5 mm by using the operator console software, and the acquisition was repeated. This procedure was repeated until the start position of the current acquisition equaled the position of the second image in the initial acquisition. In this manner, a volume with length equal to three times the scan width was imaged at 0.5-mm intervals.

This data acquisition sequence requires that the patient table position be both accurate and reproducible. Table increment (step size) and repositioning (ability to move away from and back to a specific location) are tested at least semiannually[6] on each of our institution's three electron beam CT scanners and have repeatedly performed within acceptance limits (± 1 mm). Thus, the width parameters of electron beam CT section sensitivity profiles should be accurate and reproducible, at a minimum, to within 1 mm.

All images were reconstructed using a 9-cm field of view with use of the normal CVS reconstruction mode (i.e., without use of the interpolation algorithm available in the overlapped or cone-beam reconstruction modes). Images were reconstructed primarily using the ''normal'' reconstruction kernel, although some images were reconstructed using the ''smooth'' and ''sharp'' reconstruction kernels to benchmark how changes in image noise as a result of collimator width and exposure time selection compared with the familiar effects of kernel selection. Unlike the choice of collimator width or exposure time, the choice of reconstruction kernel should not affect the section sensitivity profile.

After data acquisition and image reconstruction, the amount of bead visible within each image was determined

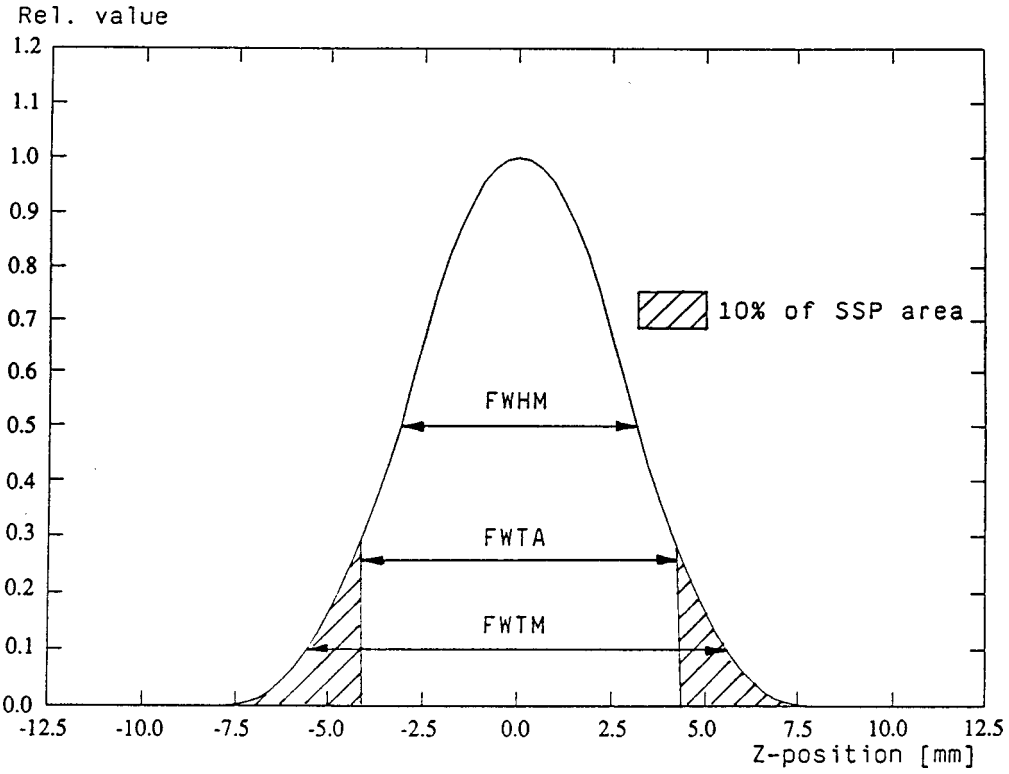

FIG. 1. Width descriptors of the section sensitivity profile (SSP). The full width at half-maximum (FWHM) typically is used to describe the nominal scan width. The FWTM is the full width at one-tenth of the maximum, and the FWTA is defined as the width between points on the profiles which include 90% of the area and exclude 10% of the area under the entire profile. [From Polacin *et al.* (Ref. 7). By permission of Radiological Society of North America.]

quantitatively by measuring the bead attenuation (image brightness or CT number, in Hounsfield units) within a small (0.37–1.14 mm^2, 12–37 pixels) circular region of interest centered on the bead. Although use of the larger region of interest (1.14 mm^2 included the bead but not the acrylic support rods) provides a lower noise estimate of the mean CT number within the region of interest, streak artifacts emanating from acrylic supports near the bead required that we occasionally reduce the size of the region of interest. The same size region of interest was used for all measurements within a given scan sequence to ensure that the amount of background attenuation included in the bead region of interest remained constant for a given profile data set. The mean CT number within this region of interest was plotted against table position to determine the section sensitivity profiles. Similarly, the mean CT number and the standard deviation about the mean were measured with a 400 mm^2 region of interest placed at the center of the water phantom images to determine image noise.

The full width at half maximum (FWHM), the full width at tenth maximum (FWTM), and full width at tenth area (FWTA) were used as descriptors of the section sensitivity profile (Fig. 1). Polacin *et al.*[7] used these descriptors to evaluate section sensitivity profiles in spiral CT. Of these descriptors, the FWHM typically is used to describe the nominal section width.

The average of the CT numbers for data points most distant to the bead, where the attenuation values fluctuated about a local minimum, was used as the profile baseline. The appropriateness of the baseline was confirmed by visual inspection of the plotted section sensitivity profile. The peak CT number within the profile, minus the baseline value, was used as the measure of maximum profile height. This maximum value was multiplied by 0.5 and 0.1 to determine the half and tenth value heights, respectively, which were then added to the baseline value to determine the target CT numbers for the half and tenth maximum heights on the profiles. The FWHM and FWTM were determined by linearly interpolating between data points bracketing the 50% and 10% target CT numbers, respectively.

The FWTA describes the full width along the z axis between the points on the profile which include 90% of the area under the profile and exclude 10% of the area under the profile. The FWTA was calculated with use of a mathematical software package (MATLAB, The Math Works, Inc., Natick, MA). With use of the baseline determined as described above, the area under the profile was calculated using the ''quad'' function (numerical integration according to Simpson's rule).[8] Beginning with the outermost points on the profile, iterative area calculations were performed using 0.1-mm z-axis intervals symmetrical about the peak of the profile. The locations that delimited an area under the profile closest to 0.9 times the maximum area were used to calculate the profile's FWTA.

To provide a visual indication of the effect of changes in the section sensitivity profile, a section thickness and contiguity phantom[9] (Fig. 2) was imaged for the 6-mm scan width

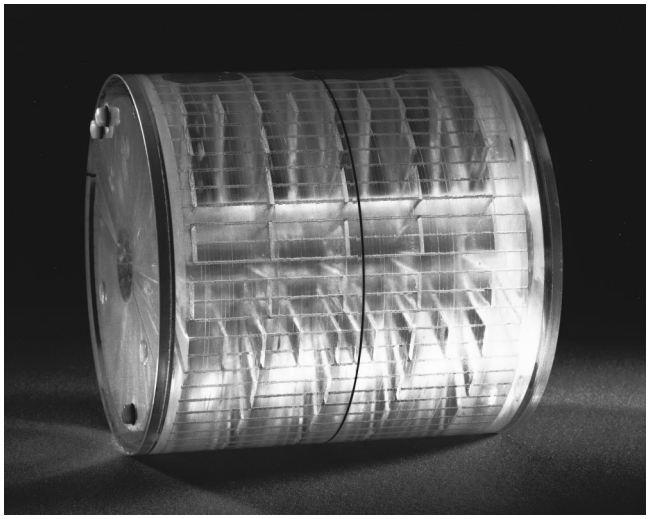

FIG. 2. The section thickness and contiguity phantom (Ref. 9) used to visually demonstrate changes in the section sensitivity profiles.

using the 6-, 3-, and 1.5-mm collimator widths and for the 3-mm scan width using the 3- and 1.5-mm collimator widths.

III. RESULTS

Table I details the FWHM, FWTM, and FWTA width descriptors and the corresponding image noise for the section sensitivity profiles measured in this study. Figure 3 shows the section sensitivity profiles for contiguous (scan width equals table increment) 6-mm scans acquired with a 0.4-s exposure time and both the SVS and the CVS acquisition modes. Figure 4 plots the FWHM, FWTM, FWTA, and image noise corresponding to the section sensitivity profiles shown in Fig. 3. The mean CT numbers measured within the uniform water phantom are not reported because none differed from 0 HU (the nominal CT number of water) by more than 5 HU. The effect of changes in the section sensitivity profiles in Fig. 3 is shown in Fig. 5. In these images, each wedge represents a 2-mm thickness along the *z* axis. Wedges that are partially visible indicate a *z*-axis contribution to the image less than 2 mm. Figure 6 compares the effect of the reconstruction kernel and exposure time on FWHM, FWTM, FWTA, and image noise.

IV. DISCUSSION

The section sensitivity profiles shown in Fig. 3 demonstrate several results that apply to all of the section sensitivity profiles measured in this study. First, the SVS mode produced the most compact section sensitivity profile. In this mode, the relative sensitivity, or image contrast, is maximized within the nominal scan width, and the ''tails,'' which extend beyond the nominal scan width, are minimized. These characteristics minimize partial volume averaging along the *z* axis. Second, in the CVS mode, the choice of collimator width significantly influenced the shape of the section sensitivity profile. Larger collimator widths produced decreased sensitivity within the central portion of the scan and caused an increase in sensitivity outside the nominal scan width (that is, wider tails). These characteristics increase partial volume averaging along the *z* axis and reduce image contrast for objects smaller than the scan width. As the collimator size was decreased, the tails of the section sensitivity profile were reduced and the sensitivity within the central portion of the scan increased. Use of the 1.5-mm collimator width produced a section sensitivity profile in the CVS mode that was closest to the ''best'' section sensitivity profile which was produced in the SVS mode.

Although the spatial characteristics of the section sensitivity profile are optimized with use of a smaller collimator width, image noise is increased with the use of a smaller collimator width (Table I and Fig. 4). This increase is caused by the decrease in the number of photons that pass through the smaller collimators. Because noise plays an important role in low-contrast visualization, this increase in image noise will detrimentally affect low-contrast visualization. The degree to which this effect counteracts the increase in contrast due to the more ideal section sensitivity profile will depend on the size of the low-contrast object. Thus, the appropriate trade-off between *z*-axis resolution (partial volume averaging) and image noise may differ for different diagnostic tasks and needs to be optimized in a clinical study. These trends with increasing collimator width (widening of the section sensitivity profile, increased partial volume averaging, and decreased image noise) were noted consistently for all CVS data.

The FWHM did not vary with collimator size in the CVS mode (Table I and Fig. 4). In all cases the FWHM was within 0.5 mm of the nominal scan width, and in most cases it was within 0.1 mm of the nominal scan width. Thus, the FWHM seems to be an insensitive measure of differences in the section sensitivity profile and does not provide the radiologist with useful information regarding changes in partial volume averaging due to changes in collimator (or other parameter) selection. The FWTM and FWTA, however, were larger for the CVS mode than for the SVS mode and increased substantially with an increase in collimator width. These descriptors of the section sensitivity profile seem to better describe the broadening that occurs in the CVS mode because they measure the tails of the profile, where the effect is greatest. Similar results regarding the relevance of the FWHM, FWTM, and FWTA were reported by Polacin *et al.*[7] for spiral CT.

The phantom images shown in Fig. 5 provide a visual estimate of the perceived image scan width. Complete visualization of a wedge (uniform maximum contrast) implies that 2 mm along the *z* axis was included in the image. Partial visualization of a wedge indicates that something less than 2 mm along the *z* axis was included in the image. Qualitative assessment of the degree of partial visualization is necessary to estimate the scan width. Although this technique is subject to some uncertainty because of the reliance on partial volume averaging and subjective assessment of image contrast, the images clearly show an increase in image width which is consistent with the measured increase in FWTM and FWTA. The scan width estimated from these images increased with use of the CVS mode and with increased collimator width

TABLE I. The full width at half maximum (FWHM), full width at tenth maximum (FWTM), full width at tenth area (FWTA), and image noise as a function of scan width, collimator width, exposure time, and reconstruction kernel for contiguous scans (scan width = table increment)

Scan width, mm	Collimator width, mm	Exposure time, s	Reconstruction kernel	No. of measurements	FWHM, mm[a]	FWTM, mm[a]	FWTA, mm[a]	Noise, HU
				CVS scan mode				
10	6	0.4	Normal	2	9.96±0.05	14.25±0.21	11.65±0.07	12.3
	3	1.4	Normal	2	9.94±0.15	12.71±0.59	10.55±0.21	9.5
8	6	0.4	Normal	2	7.46±0.40	12.03±0.04	9.90±0.42	12.1
	6	1.4	Normal	2	8.01±0.21	12.52±0.13	10.35±0.35	11.4
	3	0.4	Normal	2	7.98±0.22	10.40±0.20	8.55±0.21	14.7
	1.5	0.6	Normal	1	7.57	9.71	6.90	16.3
	1.5	1.4	Normal	2	8.06±0.14	9.38±0.16	7.85±0.21	13.2
6	6	0.4	Normal	3	6.00±0.24	10.27±0.07	8.40±0.26	11.9
	6	0.4	Smooth	1	5.82	10.20	8.70	6.8
	6	0.4	Sharp	2	5.87±0.05	10.42±0.22	8.65±0.07	19.1
	6	1.4	Normal	1	6.32	10.59	8.30	7.2
	6	1.4	Smooth	1	6.18	10.48	8.40	3.8
	6	1.4	Sharp	1	6.11	10.58	8.30	11.7
	3	0.4	Normal	2	5.88±0.04	8.38±0.34	7.00±0.14	14.9
	1.5	0.4	Normal	3	6.02±0.05	7.62±0.42	6.40±0.10	17.2
	1.5	0.4	Smooth	2	6.03±0.08	7.44±0.29	5.85±0.07	11.1
	1.5	0.4	Sharp	2	5.94±0.17	7.48±0.25	5.75±0.21	26.7
	1.5	1.4	Normal	3	5.78±0.17	7.46±0.16	6.23±0.32	12.5
3	3	0.4	Normal	2	3.37±0.01	5.31±0.27	4.10±0.00	15.0
	1.5	0.4	Normal	3	2.95±0.02	4.50±0.20	3.60±0.20	17.4
1.5	1.5	0.4	Normal	3	1.70±0.02	3.01±0.13	2.37±0.12	17.4
	1.5	1.2	Normal	3	1.67±0.06	2.98±0.04	2.30±0.00	13.3
				SVS scan mode				
6	6	0.4	Normal	3	5.93±0.11	6.95±0.05	5.67±0.21	11.9
		1.4	Normal	3	5.97±0.09	6.80±0.15	5.63±0.15	7.0
		1.4	Smooth	3	5.93±0.08	6.99±0.09	5.53±0.06	3.7
		1.4	Sharp	2	5.91±0.06	7.04±0.10	5.55±0.07	11.8
3	3	0.4	Normal	3	2.75±0.14	4.23±0.08	3.30±0.17	14.6
		1.4	Normal	3	2.69±0.02	4.18±0.06	3.40±0.10	10.0
		1.4	Smooth	3	2.77±0.10	3.85±0.30	3.20±0.26	6.4
		1.4	Sharp	2	2.86±0.07	4.03±0.08	3.40±0.00	16.0
1.5	1.5	0.4	Normal	3	1.50±0.05	2.14±0.05	1.80±0.00	17.2
		1.4	Normal	2	1.46±0.01	2.22±0.05	1.80±0.00	13.4
		1.4	Smooth	3	1.49±0.03	2.30±0.03	1.80±0.00	6.9
		1.4	Sharp	3	1.45±0.01	2.37±0.06	1.80±0.00	18.7

[a]Width values are mean (± standard deviation for multiple measurements).

and corresponded closely to the FWTM and FWTA. Thus, we conclude that the FWTM and the FWTA are better indicators of *z*-axis resolution than the FWHM.

We found that increasing CVS exposure time beyond 0.4 s, which decreases table speed, did not significantly affect the section sensitivity profile widths. This result cannot be extended to imply that there is no exposure time effect in CVS; very short exposures (0.1 or 0.2 s), which correspond to faster table speeds, require the use of interpolation algorithms similar to those used in spiral CT to reduce table motion artifacts (available in the overlapped and cone-beam reconstruction modes). As noted above, these short exposure times and reconstruction modes are less-used clinically and were not evaluated in this study. However, if used, profile widths, image noise, image artifacts, and variations in these parameters across the field of view will be affected in a manner similar to that observed in spiral CT using a similar algorithm (180° LI).[10–12]

In comparing CVS to spiral CT, it is important to note that the variations in section sensitivity profiles, image noise, and image artifacts across the field of view observed in spiral CT are not expected and have not been observed using the normal CVS mode.[12] Like spiral CT, decreasing the collimation width improves (narrows) the section sensitivity profile but increases image noise. Unlike spiral CT, in which decreasing the table speed for a given collimation width (i.e., decreasing the pitch to $\geqslant 1$) narrows the sensitivity profile but does not affect image noise, decreasing the table speed in CVS for a given collimation (by increasing the cumulative exposure time beyond 0.4 s) significantly decreases image noise but does not affect the sensitivity profile.

Although the choice of reconstruction kernel or exposure time greater than 0.4 s does not alter the characteristics of the section sensitivity profile (Fig. 6), both affect image noise. To offset the noise increase (11.9–17.2 HU) for contiguous 6-mm 0.4-s scans as the collimator width is decreased from 6 to 1.5 requires the use of a smooth kernel (noise=11.1 HU) or an exposure time of 1.4 s (noise=12.5 HU, normal ker-

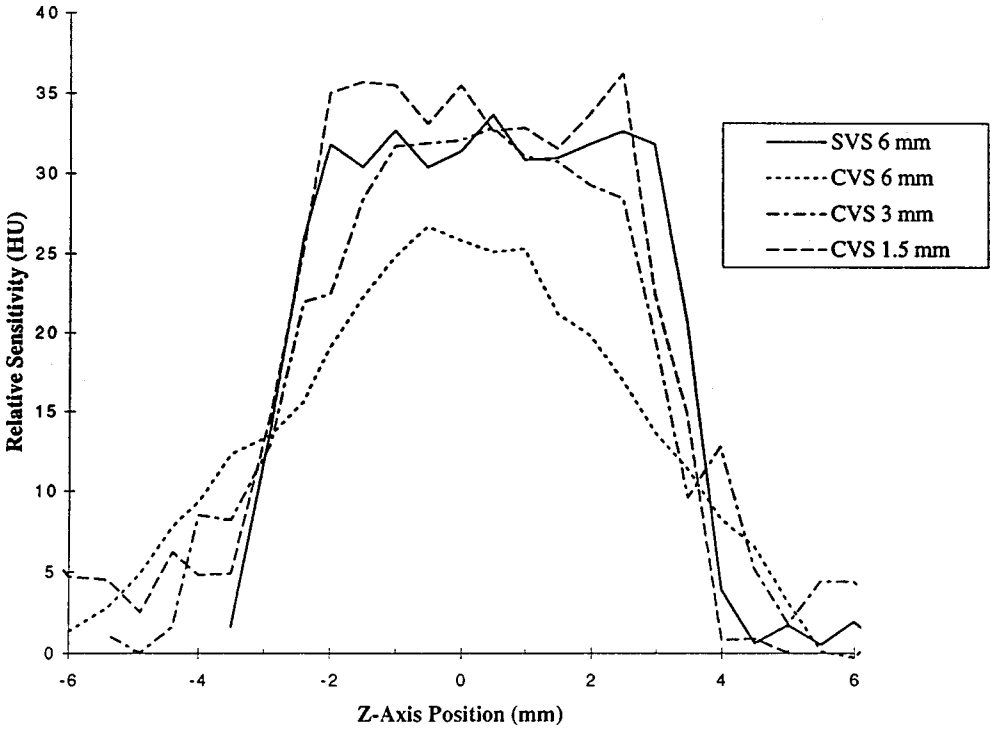

FIG. 3. Section sensitivity profiles for contiguous 6-mm-wide scans (scan width equals scan increment) acquired with a 0.4-s exposure time and the SVS and CVS acquisition modes. The values in the legend with SVS and CVS correspond to the collimator width. In the SVS mode, a 6-mm collimator width is used to acquire a 6-mm scan. In the CVS mode, a 6-mm-wide scan can be obtained with a 1.5-, 3-, or 6-mm collimator width. The most compact section sensitivity profile is obtained in the SVS mode. In the CVS mode, the use of wider collimator widths resulted in broader section sensitivity profiles, whereas the use of the smallest collimator width resulted in section sensitivity profiles that were very close to the ideal (SVS) section sensitivity profiles.

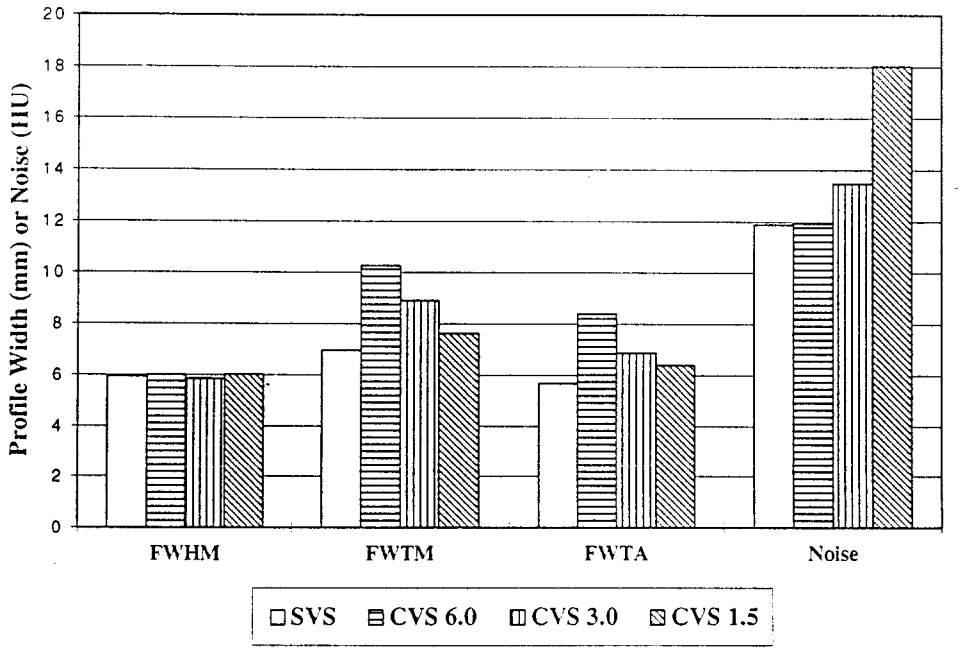

FIG. 4. Comparison of the FWHM, FWTM, and FWTA width descriptors and image noise for the section sensitivity profiles shown in Fig. 3. For each width descriptor or image noise, from left to right, data are shown for a 6-mm SVS image and contiguous 6-mm CVS images using the 6-, 3-, or 1.5-mm collimator width. All images were acquired with a 0.4-s exposure time. The FWHM changed negligibly between SVS and CVS modes, even when the collimator width was varied. The FWTM and FWTA increased in the CVS mode compared with the SVS mode and were largest for wider collimator widths. Image noise increased as the collimator width decreased.

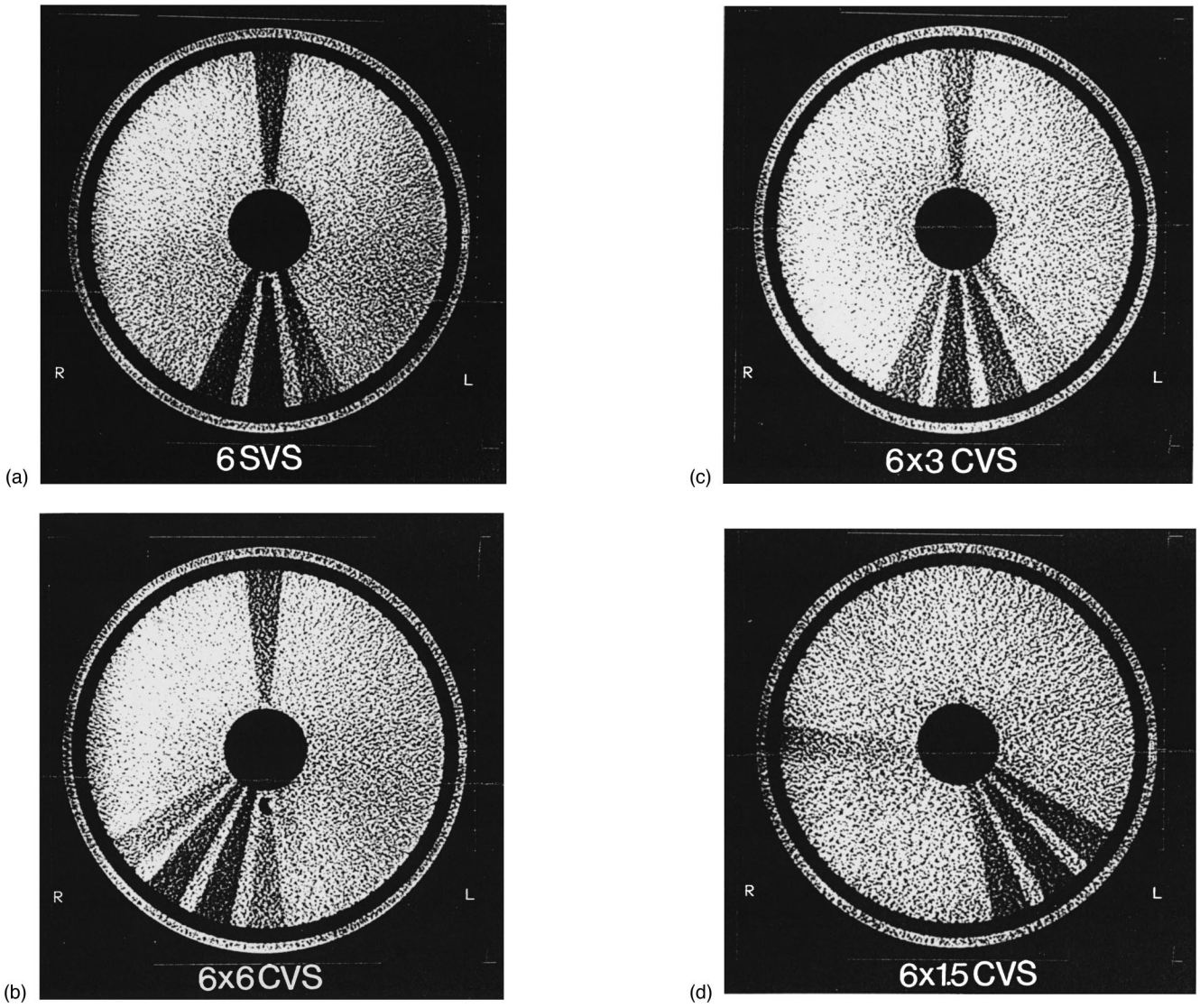

FIG. 5. Images acquired with the section thickness and contiguity phantom (Ref. 9) shown in Fig. 2. Each wedge represents 2 mm along the *z* axis. For example, three contiguous wedges having uniform and equal contrast represent a scan width of 6 mm. The solitary wedge in the upper half of the phantom is used for alignment and positioning purposes only and should be ignored. All images were acquired with a 0.4-s exposure time. (a), SVS mode, 6-mm nominal scan width. (b), CVS mode, contiguous 6-mm scans acquired with a 6-mm collimator. (c), CVS mode, contiguous 6-mm scans acquired with a 3-mm collimator. (d), CVS mode, contiguous 6-mm scans acquired with a 1.5-mm collimator.

nel). Use of the smooth kernel degrades high-frequency spatial resolution, and use of increased exposure times decreases temporal resolution and increases patient dose. Thus, an appropriate trade-off between these image quality and dose considerations must be made in relation to the clinical requirements of the examination.

Table I summarizes the FWHM, FWTM, FWTA, and image noise data acquired with the SVS and CVS modes for all parameter combinations studied. The width data shown are the mean values for one to three measurements. The standard deviation of multiple measurements, averaged over all parameter combinations, was used as an indicator of measurement precision and was found to be 0.10, 0.16, and 0.14 mm for the FWHM, FWTM, and FWTA, respectively. Thus, despite the course sampling of the section sensitivity profile (0.5 mm) necessitated by the labor-intensive data acquisition and analysis procedures, and possible table positioning errors smaller than the 1-mm detection limits of our quality assurance tests, these descriptors of the section sensitivity profile were very reproducible and provided values that can be considered accurate to within 0.5 mm. Finer sampling of the section sensitivity profile would have produced smoother curves and perhaps increased the accuracy of these quantitative descriptors. However, the method described here seems to have been sufficient to identify clinically relevant relationships between the SVS and CVS modes and for different collimator widths.

In an attempt to reduce statistical uncertainty in the measured mean CT over the bead region of interest, a larger region of interest ($2–6\ mm^2$ instead of $0.37–1.14\ mm^2$) was used for attenuation measurements in a bead phantom having more uniform surroundings (CatPhan module CTP445,

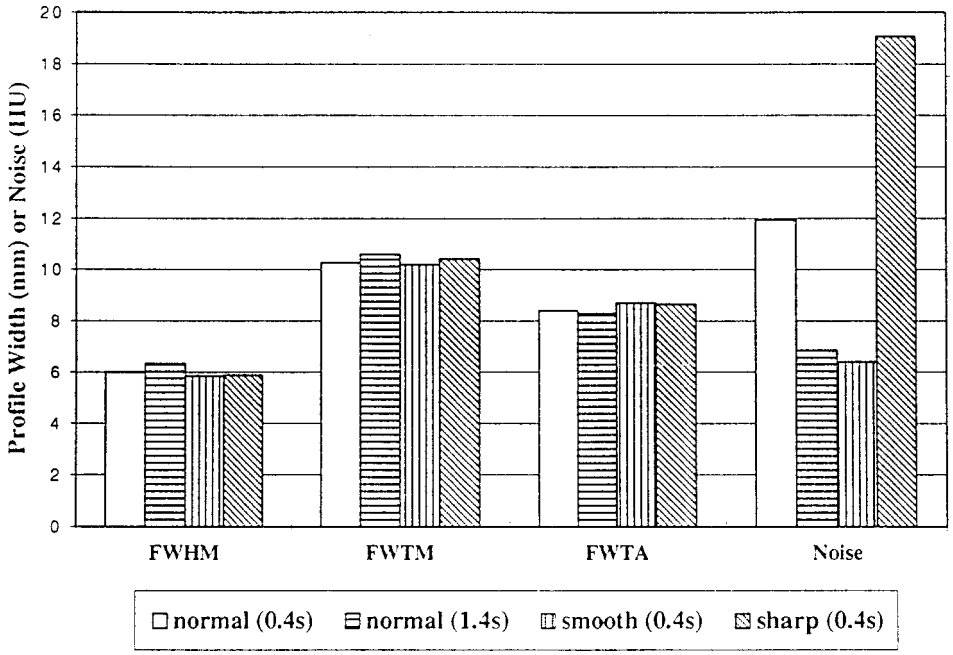

FIG. 6. Effect of the reconstruction kernel and exposure time on the FWHM, FWTM, and FWTA width descriptors and image noise. From left to right, the data represent a normal reconstruction kernel and 0.4-s exposure, normal reconstruction kernel and 1.4-s exposure, a smooth reconstruction kernel and 0.4-s exposure, and a sharp reconstruction kernel and 0.4-s exposure. Neither the reconstruction kernel nor the cumulative exposure times greater than 0.4 s have a significant effect on the width of the section sensitivity profile. However, as expected, both the reconstruction kernel and the exposure time affect image noise.

Phantom Laboratory, Stanford, CT). No significant difference in the measured section sensitivity profile descriptors was noted, although anecdotally the section sensitivity profiles appeared somewhat less noisy. This phantom, which was tested after the data for this study had been acquired, was deemed easier to use because the region surrounding the bead was extremely uniform. Thus, a larger region of interest could be used and placement of the region of interest was not critical, as was the case for the phantom used in the study (Nuclear Associates). Additionally, the CatPhan bead provided higher attenuation and thus increased the ratio of signal (bead attenuation) to image noise. The phantom was also easier to align and stabilize on the patient table.

In summary, this study provides clinically relevant information to the radiologist who must choose among various scan parameters. Whereas the FWHM of the section sensitivity profile remained essentially constant (and equal to the nominal scan width) with use of the CVS data acquisition mode, the measured FWTM and FWTA reflected the broadening of the section sensitivity profile caused by table motion. This broadening increases the sensitivity to objects outside the nominal scan width and decreases the sensitivity to objects within the nominal scan width. These changes in the section sensitivity profile reduce image contrast and increase partial volume averaging along the *z* axis. The CVS mode offers considerable clinical advantages because of the dramatic decrease in examination acquisition time (for example, 40 images can be acquired in times as short as 14 s in the CVS mode, as opposed to 52 s in the SVS mode) and is the preferred mode of operation for most applications. Thus, radiologists who use the CVS mode may want to counteract the undesirable widening of the section sensitivity profile by using smaller collimator widths. Image noise, however, is increased with the use of smaller collimator widths and may need to be offset using increased exposure times (which reduces temporal resolution and increases patient dose) or a smoother kernel (which degrades spatial resolution). The appropriate trade-off between image noise and *z*-axis resolution and the effect of parameter selection on perceived anatomical image quality and diagnostic efficacy will depend on object size and composition. Thus, further study using clinically relevant low-contrast lesions is warranted.

ACKNOWLEDGMENTS

The authors acknowledge the expert assistance of Timothy R. Daly, R.T. (R), in data collection and Frank E. Zink, Ph.D., in manuscript review. We also thank Nuclear Associates and Phantom Laboratory for allowing us to borrow their phantoms during the course of this study.

[a]Nothing in this publication implies that Mayo Foundation endorses the products of Nuclear Associates or Phantom Laboratory.

[b]Address reprint requests to: Dr. McCollough, Mayo Clinic, 200 First Street SW, Rochester, MN 55905; electronic mail: mccollough.cynthia@mayo.edu

[1]D. P. Boyd, ''Transmission computed tomography,'' in *Radiology of the Skull and Brain: Technical Aspects of Computed Tomography*, edited by T. H. Newton and D. G. Potts (Mosby, St. Louis, 1981), Vol. 5, pp. 4357–4371.

[2]D. P. Boyd, ''Computerized transmission tomography of the heart using scanning electron beams,'' in *CT of the Heart and the Great Vessels: Experimental Evaluation and Clinical Application*, edited by C. B. Higgins (Futura, Mount Kisco, New York, 1983), pp. 45–60.

[3]W. Stanford and J. A. Rumberger, *Ultrafast Computerized Tomography in Cardiac Imaging: Principles and Practice* (Futura, Mount Kisco, New York, 1992), pp. 1–22.
[4]C. H. McCollough and R. L. Morin, ''The technical design and performance of ultrafast computed tomography,'' Radiol. Clin. North Am. **32**, 521–536 (1994).
[5]C. H. McCollough, ''Principles and performance of electron beam CT,'' in *Medical CT and Ultrasound: Current Technology and Applications*, edited by L. W. Goldman and J. B. Fowlkes (Advanced Medical Publishing, Madison, Wisconsin, 1995), pp. 411–436.
[6]C. H. McCollough and F. E. Zink, ''Quality control and acceptance testing of CT systems,'' in *Medical CT and Ultrasound: Current Technology and Applications*, edited by L. W. Goldman and J. B. Fowlkes (Advanced Medical Publishing, Madison, Wisconsin, 1995), pp. 437–465.
[7]A. Polacin, W. A. Kalender, and G. Marchal, ''Evaluation of section sensitivity profiles and image noise in spiral CT,'' Radiology **185**, 29–35 (1992).
[8]G. E. Forsythe, M. A. Malcolm and C. B. Moler, *Computer Methods for Mathematical Computation* (Prentice–Hall, Englewood Cliffs, NJ, 1977).
[9]J. E. Gray and J. P. Felmlee, ''Section thickness and contiguity phantom for MR imaging.'' Radiology **164**, 193–197 (1987).
[10]G. Wang and M. W. Vannier, ''Longitudinal resolution in volumetric x-ray computerized tomography: Analytical comparison between conventional and helical computerized tomography,'' Med. Phys. **21**, 429–433 (1994).
[11]G. Wang and M. W. Vannier, ''Helical CT image noise: Analytical results,'' Med. Phys. **20**, 1635–1640 (1993).
[12]G. Wang and M. W. Vannier, ''Spatial variation of section sensitivity profile in helical computed tomography,'' Med. Phys. **21**, 1491–1497 (1994).